Enhancing Corrosion Resistance of Stainless Steel 304 Using Laser Surface Treatment

I.M. Ghayad[1]*, M.A. Shoeib[2], T. Mattar[2], R.M AbuShhaiba[2] and H.M. Hussein[2]

[1]Faculty of Science, AlAzhar University, Cairo, Egypt

[2]Central Metallurgical Research and Development Institute, P.O. Box: 87, Helwan, Cairo, Egypt

Abstract

Stainless steel AISI 304 was laser treated to enhance corrosion resistance and improve surface properties. This alloy has many applications in auto industry (car body) as well as oil and gas industry. Different conditions were applied in the laser surface treatment, namely: laser power density, scan speed, distance between paths, medium gas (air, argon and nitrogen). After laser treatment, the samples microstructures were investigated using optical microscope to examine microstructural changes due to laser irradiation. Specimen surfaces were investigated using XRD, SEM and EDAX before and after laser treatment to examine the surface composition changes brought by laser irradiation. Results showed that laser irradiation enhances the corrosion resistance of AISI 304 Stainless steel to a large extent. Corrosion rates as low as 0.011 mpy for laser treated samples were obtained in comparison to 0.952 mpy obtained for the untreated samples. Superior pitting corrosion resistance was obtained under specific treatment conditions. The enhancement of corrosion resistance depends on the laser irradiation conditions. The corrosion protection afforded by laser treatment is attributed mainly to the grain refinement of the top surface layer. This layer is found to consist of nano-scale grains.

Introduction

The laser treatment of metals and alloys has emerged as a novel surface modification technique, and laser application in the surface treatment has grown rapidly in recent years [1-14]. There are some fields where laser surface treatments have an important chance such as aerospace components, automobile applications and oil and gas industries. The evolution of laser treatments has been focusing on the modification of corrosion and wear resistance for new applications.

Owing to a number of special features, laser treatment has emerged as a popular technique in surface modification. Laser surface modification derives its attractiveness in engineering applications from [1]:

1. The formation of a small heat-affected zone, thus leaving the bulk properties unchanged and introducing minimal distortion;
2. Refinement and homogenization of microstructure, leading to enhanced mechanical properties and corrosion resistance;
3. The possibility of forming novel surface alloys unattainable by other methods because of the non-equilibrium nature of the process.

In the case of iron, it has been shown that laser irradiation in air or nitrogen atmospheres can lead to significant surface nitration [2], which is known to improve the hardness and corrosion resistance of the surface materials. Since, at sufficiently high power, the laser beam induces melting and vaporization of metals, chemical composition (depending on the ambient atmosphere), structure and morphology are modified, leading to a change in the surface characteristics. It was shown that the laser irradiation of iron surfaces in air causes the incorporation of oxygen and nitrogen deep in the thickness. Moreover, the initial α-Fe phase is partly transformed into oxide and nitride ones. In order to gain more insight into chemical and crystalline structure modifications, treatments were performed using different kinds of laser beams [2-4].

*corresponding author. E-mail: dr_ghayad@yahoo.com

Printed in Kazakhstan

Pereira *et al.* [3] studied the steel surface modifications induced by irradiation of several lasers in air. The surface modifications are found to depend on the laser properties. The treated surface features are analyzed. It was concluded that carbon coming from the machining oils is successfully removed under all the studied conditions, the incorporation of oxygen and nitrogen (beyond 1 mm in depth) to the surface occurred. In addition to the original ferrite phase, new crystalline compounds are detected after treatment such as austenite, oxides (FeO or FeO, FeO) and nitride. Depending on the laser characteristics, the main formed crystalline phases are different (oxide or nitride). Under some experimental conditions, the formation of a back deposition layer composed of oxides and hydroxides is observed.

According to Kac and Kusinski [5], the steep temperature gradients and high solidification rates associated with localized, rapid surface melting when using pulsed Nd:YAG radiation can lead to the easy formation, during solidification process, of ultrafine eutectics in the ASP2060 high-speed tool steel with a high microstructural and chemical homogeneity. This in turn reveals different features of hardening (occurring during rapid post-solidification quenching of sample to room temperature), and as a consequence changes significantly the microstructure and mechanical properties of the laser resolidified surface layer in comparison to conventionally hardened matrix. Indeed, such metallurgical changes that occurred in the laser-modified layer, which are in the forms of grain refinement, supersaturated solid solutions, and fine dispersions of particles can contribute to the hardening and strengthening of the surface layer. Kac and Kusinski results are summarized as follows: The surface layers obtained after Nd:YAG laser melting was relatively smooth, morphologically homogenous without presence of cracks and porosity. The central and surface part of the laser-melted zone possessed an ultrafine grain structure. The substructure of these grains consists of very fine dendritic eutectics.

Conde *et al.* [6] showed that the laser surface melting (LSM) of 304 SS in argon and nitrogen atmospheres induced improvements in pitting resistance with respect to the base steel. Electrochemical studies showed that the improvements are greater when the LSM is carried out in a nitrogen environment because of the incorporation of nitrogen into solid solution. As a result, the corrosion and pitting potential shift to more noble values while the passive current density decreases by nearly two orders of magnitude. The presence of chromium oxides and nitrogen compounds on the surface of the specimens seem to indicate that nitrogen may help the reconstruction of the passive layer as well as act as a barrier for the electrolyte.

The aim of the present paper is to study the effect of laser surface treatment on the corrosion resistance, microstructure and surface properties of the irradiated AISI 304 stainless steel alloy.

Experimental

Materials

In performing the investigation of the effect of laser surface treatment on the microstructure and corrosion behavior of AISI 304 stainless steel, whose composition is shown in Table 1, coupons of 20×30×3 mm were used as the testing specimens.

Laser treatment process was carried out using Nd-YAG diode pumped laser with maximum output power 2200 W. Laser processing parameters are shown in Table 2.

Surface Investigations

For surface investigations, cross sections were made in the plane perpendicular to the treated surface. The samples were polished and etched for the purpose of microstructure investigations using optical microscope. Scanning electron microscopic examinations (SEM) and electron dispersive X-Ray (EDX) analysis were also performed.

Electrochemical Corrosion Testing

Linear polarization and pitting corrosion tests were performed on the laser treated as well as on the untreated specimens. All tests were carried out using Autolab PGSTAT 30 specified for electrochemical measurements.

A conventional three-electrode cell of 250 ml capacity was used with platinum as a counter electrode. The working electrode was AISI 304 stainless steel

Table 1
The chemical composition of used steel grades (wt.%)

Chemical composition, wt.%									
C	Si	Mn	P	S	Cr	Mo	Ni	Al	Fe
0.08	1.1	0.5	0.022	0.025	18-20	0.1	8-10	–	Bal.

Table 2
Laser processing parameters AISI 304 stainless steel

Specimen No	Medium Gas	Gas Pressure, l/min	Laser Power, W	Scan Speed, cm/min	Distance between paths, mm	Spot diameter, mm
S1A	Air	5	130	50	3	2
S2A	Air	5	130	80	1	2
S3A	Air	5	150	100	1	2
S4A	Air	5	150	120	1	2
S5A	Air	5	200	400	1	2
S6A	Air	5	200	500	1	2
S7A	Air	5	200	600	1	2
S1N	N_2	5	1000	150	3	2
S2N	N_2	5	1000	200	3	2
S3N	N_2	5	1000	300	3	2
S4N	N_2	5	1000	350	3	2
S5N	N_2	5	1000	400	3	2
S6N	N_2	5	1000	365	3	2
S7N	N_2	10	1000	265	3	2
S8N	N_2	20	1000	265	3	2
S9N	N_2	25	1000	265	3	2
S10N	N_2	25	1800	30	3	2
S11N	N_2	25	1800	20	3	2
S1Ar	Ar	10	1800	400	3	2
S2Ar	Ar	10	1800	200	3	4
S3Ar	Ar	10	1800	100	3	4
S4Ar	Ar	10	1800	50	3	6
S5Ar	Ar	10	1800	100	3	6
S6Ar	Ar	10	1800	30	3	6

specimens treated with laser with an exposed area of 1 cm^2. All potentials were measured with respect to silver/silver chloride reference electrode (Ag/AgCl). The electrolyte consisted of 3.5% NaCl solution made up from distilled water and reagent grade NaCl (Fisher scientific). Experiments were carried out at room temperature.

Linear Polarization

Linear polarization technique was carried out by subjecting the working electrode to a potential range of 25 mV below and above corrosion potential (E_{corr}) at a scan rate of 0.1 mV/sec. The corrosion current (I_{corr}) and hence the corrosion rate (CR) can be related to the slope of the potential *vs.* current plot ($\Delta E/\Delta I$), known as the polarization resistance (R_P) and simply by $I_{corr} = B/R_{P,}$ where B is a constant.

Pitting Corrosion

Pitting corrosion experiments were performed using cyclic anodic polarization technique. In this technique, specimens were subjected to a potential

scan in the positive direction at a rate of 1 mV/sec starting at a potential slightly negative to the corrosion potential (E_{corr}). The scan is reversed at an applied current density of 1 mA/cm^2. Parameters such as: break down potential (E_b) [potential at which the current density starts to increase indicating the dissolution of the passive film, protection potential, E_p, (potential at which the current density is almost zero indicating the restoration of the passive film). The metal resistance to pitting corrosion is increased as E_b & E_p are increased.

Results and Discussion

In the AISI 304 stainless steel laser treatment experiments. It was planned to examine several parameters on the performance of the treated samples. These parameters include: Type of gas shield (oxygen, nitrogen and argon), laser power, scan speed and path length (distance between successive paths). The treated specimens are classified according to the type of gas shield. In the first group, treated under air, laser treatment was performed on 1mm thickness 304 SS. In theses experiments laser acted as a tool for heat treatment. Laser paths represent yellow tracks on the specimen surface. Under such conditions no surface melting, considered as an essential condition for the improvement of 304 SS performance, was obtained.

In the second group, treated under nitrogen, laser treatment was performed to obtain surface melting. This was obtained by using high power and low scan speed. Figure 1 shows the optical photograph of theses specimens. A zigzag surface was obtained which occurred due to the overlapping between adjacent paths. At the overlapped areas, deeper surfaces were obtained resulting in the zigzag structure. The problem of zigzag structure was overcomed in the third group, treated under argon, of specimen treated under argon, spot diameter of the laser ray was increased from 2 mm to 4 and 6 mm. This results in a flat surface (Fig. 1).

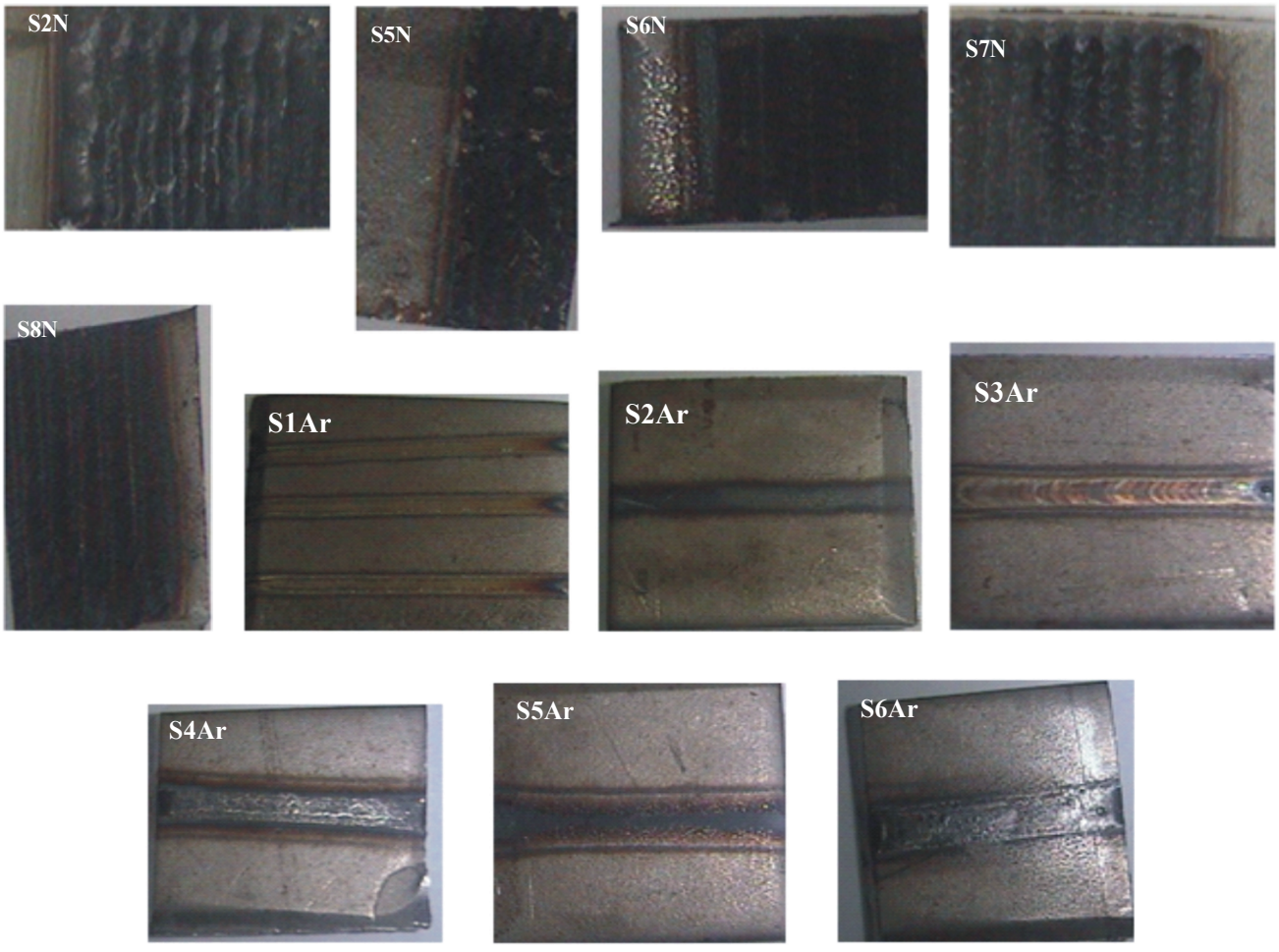

Fig. 1. Optical photographs of laser treated 304 SS specimens.

Optical Microscopy

AISI 304 stainless steel specimens' microstructures show three different zones; base metal, laser affected zone and a surface formed layer, which are clear and easily distinguishable. Representative samples were selected to represent the microstructural changes due to laser irradiation. Figure 2 shows that the base metal is composed of large grains while the surface treated layer, which is thin layer, represents hard ultrafine homogeneous structure. In a good agreement with Kac *et al.* [5], in the LSM, the liquid metal is quenched while it is in contact with the cold substrate where the steep temperature gradients and high solidification rates with localized rapid surface melting. This can lead to the formation of some materials amorphous phases with fine microstructure and high homogeneity. This observation applicable for all laser treated samples at different conditions. Figure 3 clarifies the three zones mentioned above. It is shown that the laser treated zone has a more fine structure than the base metal. As it is clear from the different micrographs, the surface treated layer is fused and rapidly solidified to form finer grains than the untreated zone (sample). In some cases an oriented dendrite structure was obtained, these results are in good agreement with Kac [4]. Because of the fusion process, the adjacent layer is affected and gains heat which in turn result in a quasi-annealing process and the cooling is slow, so a big grains microstructure is expected which the case is obtained (Fig. 3b). Other samples show the same behavior (Figs. 4, 5).

The obtained microstructure for samples, under nitrogen and argon applying different laser treatment conditions, is a fine grains surface layer followed by very big grains layer and finally the interior layer with the same grain size of untreated samples.

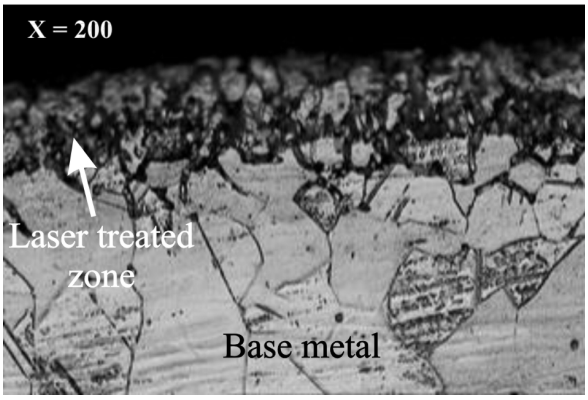

Fig. 2. Optical Microscopic photographs of sample S4Ar cross section.

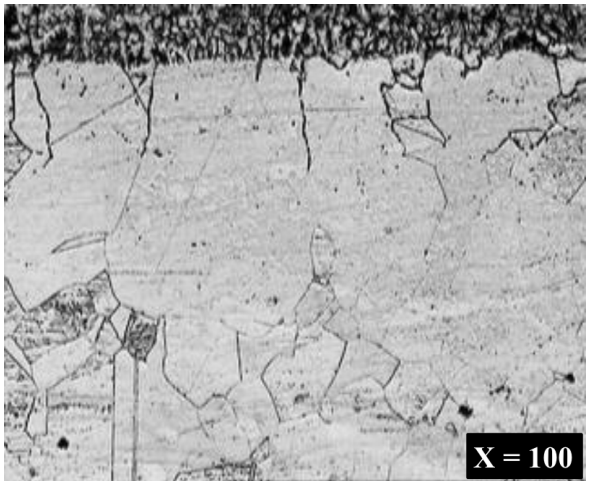

Fig. 3. Optical Microscopic photographs of sample S6Ar cross section.

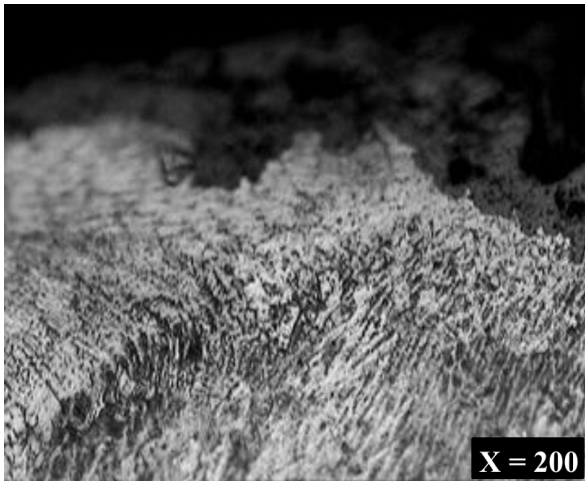

Fig. 4. Optical Microscopic photographs of sample S2N cross section.

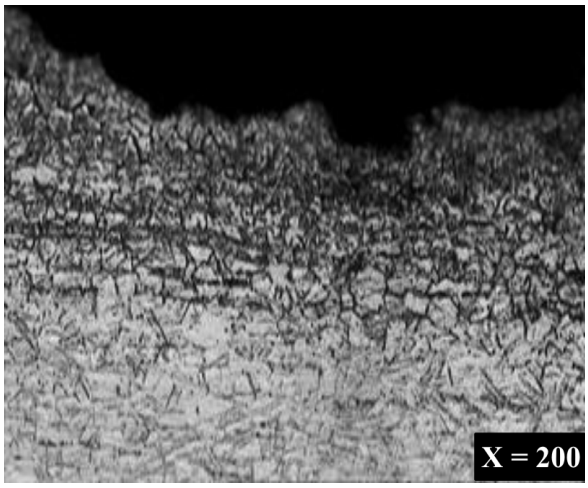

Fig. 5. Optical Microscopic photographs of sample S9N cross section.

Scanning Electron Microscopic Examination

Figure 6 shows the SEM micrograph of AISI 304 stainless steel sample S4Ar surface. It compares the grain size of the laser affected zone with the bulk of the alloy for the same specimen. It is clear that, the laser treated zone shows quite smaller grains than the bulk.

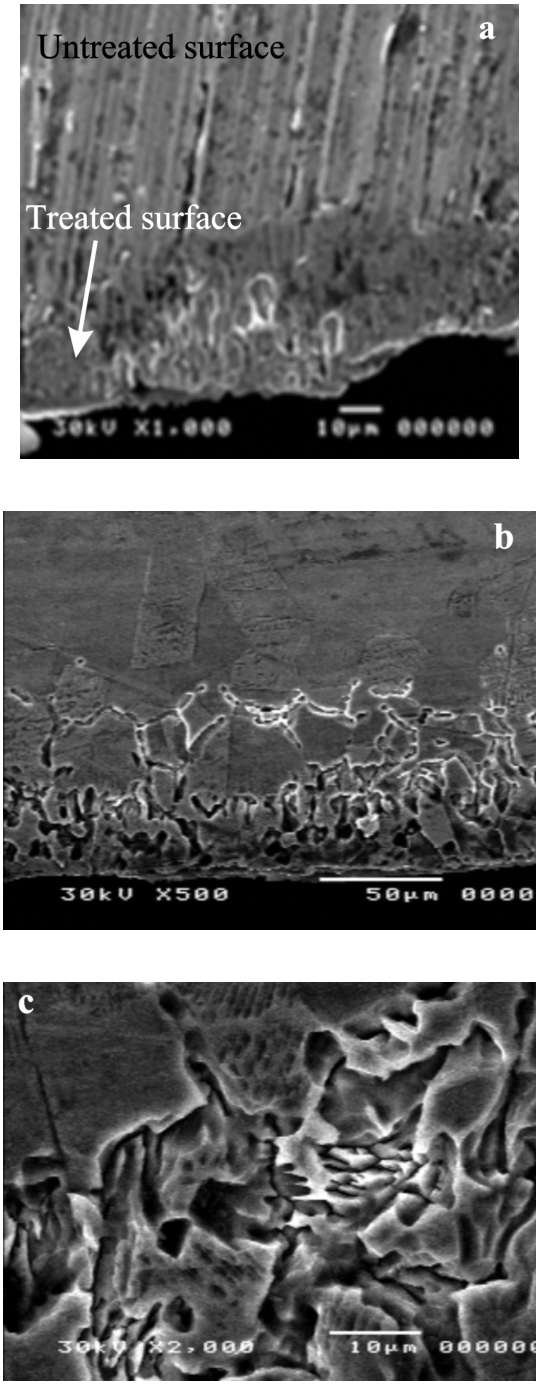

Fig. 6. SEM micrographs of cross-section of S4Ar polished and etched.

The EDAX analysis of the surface are shown in Table 3. It is typical of 304 SS. There was no N (coming from surroundings) detected on the surface which disagree with the literature [11]. This may come from the fact that N is incorporated on the very outermost layer (nanoscale layer) while the EDAX analysis depends on Electron Beam Penetration the sub surface layer (few microns depth). The surface laser affected zone is several microns in depth as it is clear from the SEM micrographs.

Table 3
EDX analysis of laser treated specimens

Specimen No	Si, %	Fe, %	Cr, %	Ni, %	Mo, %
S4 inside	0.98	75.95	15.91	6.88	0.28
S4	0.65	77.60	15.54	5.94	0.26
S6	1.91	63.12	21.61	13.36	

Corrosion Behavior of the Laser Treated Specimens

Corrosion Rate Determination Using Linear Polarization Technique

Table 4 shows the results of linear polarization experiments. In spite of the fact that the blank shows a low value of corrosion rate, laser treated samples under some conditions give lower corrosion rates in comparison to the untreated specimens. All samples treated under nitrogen and argon showed lower corrosion rates than the blank. Corrosion rates as low as 0.011 mpy (S5N) was obtained in comparison to 0.9 mpy obtained for the blank. The enhancement of corrosion resistance of the laser treated samples can be attributed to the grain refining brought by laser treatment which in turn gives a more protective film against corrosion.

Pitting Corrosion

It is well known that the major corrosion problem that faces 304 SS and stainless steel alloys in general is pitting corrosion. 304 SS suffers from pitting corrosion in chloride containing environments. Chloride ions with their small size can penetrate the protective film on the alloy in certain weak points allowing pitting corrosion to occur. The aim of laser surface treatment to improve the surface characteristic of the alloy and creating a homogeneous protective film. Cyclic

Table 4
Results of linear polarization experiments

Specimen No	E_{corr}, V	R_p, Ω·cm^2	I_{corr}, A/cm^2	CR, mpy
S0 (Blank)	-0.323	8.648E+3	3.2024	0.9521
S1A	-0.235	7.485E+3	3.6999	1.100
S2A	-0.082	1.241E+4	2.227	0.661
S6A	-0.297	8.416E+3	3.29067	0.97832
S7A	-0.313	3.052E+3	9.07414	2.6977
S2N	-0.414	2.557E+5	1.0831E-2	3.22E-3
S3N	-0.237	1.858E+5	0.14905	0.04431
S4N	-0.349	2.107E+5	0.13144	0.0391
S5N	-0.290	5.458E+4	0.50741	0.15085
S6N	-0.442	7.014E+5	0.03948	0.011739
S7N	-0.338	5.239E+5	0.052862	0.015716
S8N	-0.188	2.782E+4	0.9955	0.29596
S9N	-0.231	1.867E+4	1.48336	0.441
S10N	-0.290	3.645E+4	0.7598	0.2259
S11N	-0.286	7.582E+4	0.3653	0.1086
S4Ar	-0.207	9.672E+4	0.28633	0.08513
S6Ar	-0.275	1.243E+4	2.22802	0.6624

anodic polarization experiments, the standard technique for studying pitting corrosion, were performed on 304 SS under different conditions of laser treatment.

Figure 7 shows the pitting corrosion behavior of laser treated specimens under air. Only S2A and S4A show better behavior compared to the blank (*B*). Although these samples give nearly the same pitting potential as blank, the passive current is shifted towards more noble values and E_{corr} towards more positive values. Other specimens do not show improvement in pitting corrosion compared to the blank. As specimens were treated in air (containing oxygen) which allows the growth of an oxide layer. The combination of laser power and scan speed (130 W & 80 cm/min for S2A and 150 W & 120 cm/min for S4A) are the two factors expected to exert this improvement.

Figure 8 shows the pitting corrosion behavior of laser treated specimens treated in N_2. None of samples show a better behavior than the blank. All samples reaches a limiting current value of about 1 mA which is quite high to be considered as a passive current

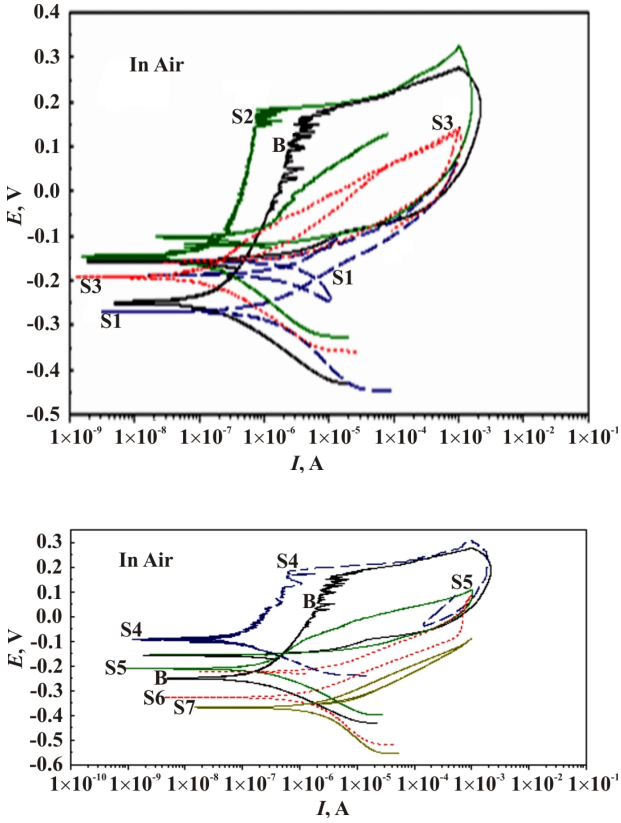

Fig. 7. Pitting corrosion behavior of laser treated AISI 304 SS under air.

(should be less than 0.1 mA). In spite of the fact that laser surface treatment of 304 SS under nitrogen enhance its pitting corrosion resistance [6], it does not exert any improvement here. It is thought that the factor causes this negative effect was the path length which was small to allow the overlapping between paths. This overlapping results in the formation of zigzag structure and no homogeneous surface was obtained.

Figure 9 shows the pitting corrosion behavior of specimens treated under argon atmosphere. Superior corrosion resistance was obtained for sample S4Ar. This is shown by the appearance of a very well defined passive region (> 1.5 V) compared to a small one given by the blank (< 0.5 V). Upon reverse of scan potential, no loop is obtained for S4 compared to a well defined loop obtained by the blank.

The results of pitting corrosion experiments show that improvement in pitting resistance of 304 SS can be obtained under specific treatment conditions. The treatment conditions play the key rules are; Type of shielding gas, scan speed and spot diameter. In the first group of specimens (treated under air), no surface melting was obtained. The used laser power was insufficient to cause melting of the surface. In the

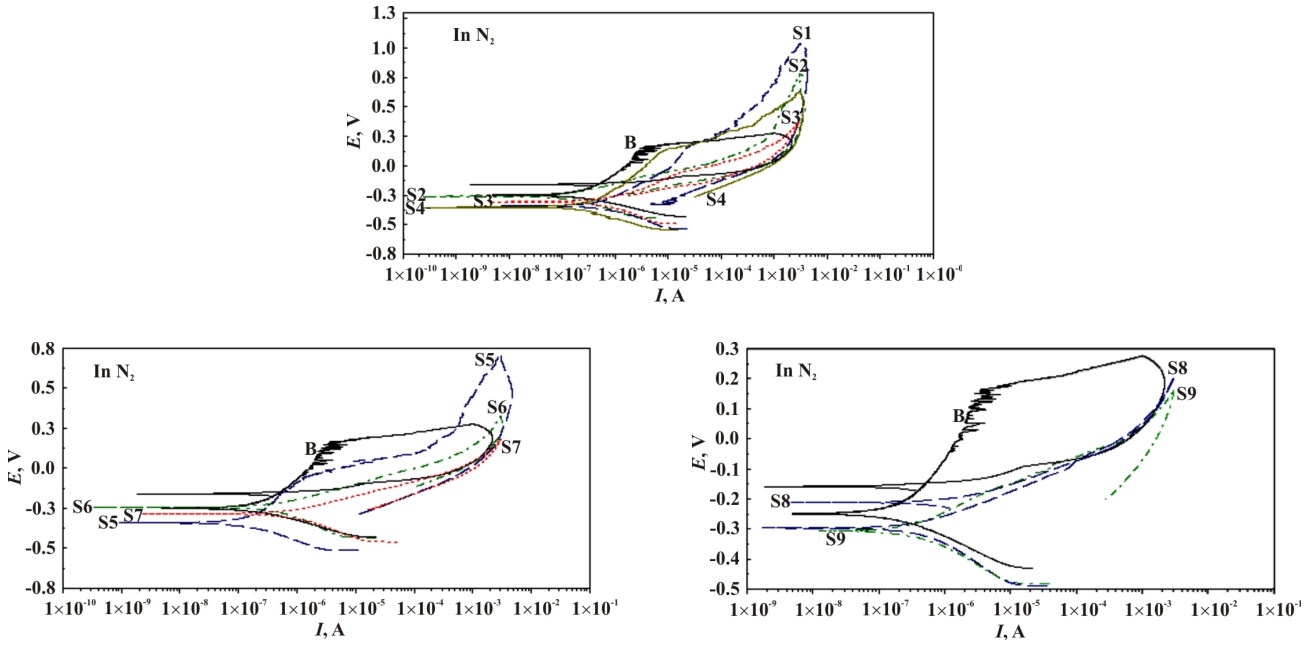

Fig. 8. Pitting corrosion behavior of laser treated AISI 304 SS under nitrogen.

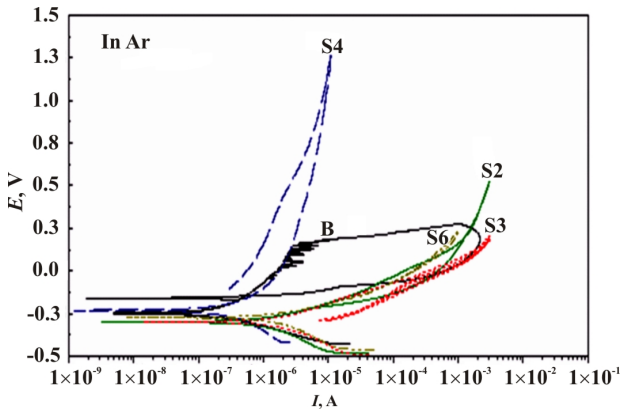

Fig. 9. Pitting corrosion behavior of laser treated AISI 304 SS under argon.

case of stainless steel, unless high power of laser is induced on the surface, there are no pronounced results could be obtained. This was obtained in this study in the second and third groups treated under nitrogen and argon respectively. However; this is not the only condition to be considered. After attaining surface melting, the important parameter considered is the spot size. Using small spot size (~ 2 mm) will lead to narrow scanned paths and overlapping between paths will be unavoidable. This case was clear with specimens treated under nitrogen atmosphere. These specimens showed zigzag shapes after laser treatment. This was obtained because the overlapped areas were twice treated by laser. This problem was avoided in the third group specimens (treated under argon). Under this condition, a flat melted surface was obtained. One of those specimens treated under argon (S4Ar) showed superior pitting and corrosion resistance. The passive current for this specimen was in the order of 10^{-6} A·cm^{-2} with a very wide passive region of potential and compared to that of the untreated or any other treated specimens. It is suggested that scan speed played the great rule. A 50 m/min was used foe S4Ar which leads us to thought that this speed is optimum to give the desired surface melting. Lower or higher scan speed may cause undesirable effects during surface melting process.

Conclusions

Laser surface treatment of stainless steel has no appreciable changes on the surface characteristics of the alloy unless high laser power is induced on the alloy surface. This high power causes the surface melting which causes the desired changes.

Laser surface melting of 304 SS brought a highly marked change in the surface morphology of the treated specimens. Grain refinement was evidenced by both optical and scanning microscoping investigations.

In the present study, superior pitting resistance was obtained for specimen treated under nitrogen using a laser power of 1800 W, 50 cm/min scan speed and 6 mm spot diameter of the laser beam. The high power causes the surface melting, the large spot diameter results in the obtaining of a flat surface and this scan speed gives the desired melting.

Laser power, laser scan speed, path length (distance between successive paths) and the spot diameter are the main factors play the big role in modifying the surface. Adaptation of these parameters together can exert the desired surface changes.

Acknowledgements

This research project is conducted via the fund of the Academy of Scientific Research and Technology, Egypt, Industrial Research Council. The experimental work was carried out in Central Metallurgical Research and Development Institute, El-Tabeen, Cairo, Egypt. The research team would like to express their great thanks to Professor M. Nasr, Director of CMRDI and colleagues in the laser unit in CMRDI for their cooperation.

References

1. C.T. Kwok, H.C. Man, F.T. Cheng, Surf. Coat. Technol. 99:295 (1998).
2. A.C. Agudelo, J.R. Gancedo, J.F. Marco, M.F. Creus. E. Gallego-Lluesma, J. Desimoni, R.C. Mercader, Appl. Surf. Sci. 148:171 (1999).
3. A. Pereira, A. Cros, P. Delaporte, W. Marine and M. Sentis, Appl. Surf. Sci. 208-209:417 (2003).
4. A.Pereira, P. Delaporte, M. Sentis, A. Cros, W. Marine, A. Basillais, A.L. Thomann, C. Leborgne, N. Semmar,P. Andreazza and T. Sauvage, Thin Solid Films 453-454:16 (2004).
5. S. Kac, J. Kusinski, Surf. Coat. Technol. 180-181:611 (2004).
6. A. Conde, I. García and J. J. de Damborenea, Corros. Sci. 43:817 (2001).
7. C.T. Kwok, F.T. Chenga, H.C. Manb, Mater. Sci. Eng. A290:55 (2000).
8. K.G. Watkins, Z. Liu, M. McMahon, R. Vilar, M.G.S. Ferreira, Mater. Sci. Eng. A252:292 (1998).
9. J. Dutta Majumdar, R. Galun, B.L. Mordike, I. Manna, Mater. Sci. Eng. A361:119 (2003).
10. R.D. Granata, P.O. Moore, in Metals Handbook, Corrosion, Vol. 13, American Society for Metals, 1985, p. 501.
11. C.C. Huang, T.W. Tsai, J.T. Lee, Corros. Sci. 37:769 (1995).
12. C.T. Kwok, F.T. Cheng, H.C. Man, Mater. Sci. Eng. A290:55 (2000).
13. C.T. Kwok, F.T. Cheng and H.C. Man, Surf. Coat. Technol. 107:31 (1998).

Received 13 February 2007.